Ecotoxicological effects of transformed silver and titanium dioxide nanoparticles in the effluent from a lab-scale wastewater treatment system

Anastasia Georgantzopoulou[†]*, *Patricia Almeida Carvalho*[‡], *Christian Vogelsang*[†], *Mengstab Tilahun*[†], *Kuria Ndungu*[†], *Andy M. Booth*[□], *Kevin V. Thomas*[†,‖] *and Ailbhe Macken*[†]

[†]NIVA, Norwegian Institute for Water Research, Gaustadalleen 21, 0349, Oslo, Norway

[‡]SINTEF Materials and Chemistry, Forskningsveien 1, 0373, Oslo, Norway

[□]SINTEF Ocean, Brattørkaia 17C, 7010, Trondheim, Norway

[‖]Queensland Alliance for Environmental Health Sciences (QAEHS), University of Queensland, 20 Cornwall Street, Woolloongabba, Queensland, 4102 Australia

ABSTRACT

In this study, a lab-scale wastewater treatment plant (WWTP), simulating biological treatment, received 10 µg/L Ag and 100 µg/L TiO_2 nanoparticles (NPs) for five weeks. NP partitioning was evaluated by size fractionation (>0.7 µm, 0.1-0.7 µm, 3 kDa-0.1 µm, <3 kDa) using inductively coupled plasma mass spectrometry (ICP-MS), single particle ICP-MS and transmission electron microscopy. The ecotoxicological effects of the transformed NPs in the effluent were assessed using a battery of marine and freshwater bioassays (algae and crustaceans) and an *in vitro* gill cell line model (RTgill-W1). TiO_2 aggregates were detected in the effluent, while Ag NPs (0.1 to 0.22 µg/L) were associated with S, Cu, Zn. Fractionation showed that >80% of Ag and Ti were associated with the effluent solids. Increased toxicity was observed during weeks 2-3 and the effects were species-dependent; with marine epibenthic copepods and algae being the most sensitive. Increased reactive oxygen species formation was observed *in vitro* followed by an increase in epithelial permeability. The effluent affected the gill epithelium integrity *in vitro* and impacted defense pathways (upregulation of multixenobiotic resistance genes). To our knowledge, this is the first study to combine a lab-scale activated sludge WWTP with extensive characterization techniques and ecotoxicological assays to study the effects of transformed NPs in the effluent.

INTRODUCTION

The production and use of consumer products containing Ag and TiO_2 NPs continues to increase[1,2] and due to their widespread use and application they can enter sewage streams and wastewater treatment plants (WWTPs). Their presence in the influent of WWTPs has been reported in several studies[3–7]. Ag and TiO_2 NPs tend to be associated with particulate matter and appear to be relatively efficiently removed from the wastewater during primary and secondary treatment[3,4,6,8,9], the extent of removal however depends on the design and efficiency of the operating conditions[6]. Ag-based and TiO_2 NPs have been detected in wastewater effluents[6,9] making their release in surface waters through effluent discharge possible, which can potentially be an important exposure route for aquatic organisms in receiving waters.

Nanoparticles undergo a combination of physical and chemical transformations in environmental media (e.g. wastewaters)[10] that may influence their behavior, bioavailability and toxicity[11,12]. Their behavior may differ from their pristine NP counterparts, thereby making comparisons and predictions between transformed and pristine NPs difficult. It has been reported that Ag NPs are sulfidized to various degrees in wastewater streams and during transport to WWTPs[8,13]. Furthermore, studies using a pilot WWTP fed with municipal wastewater spiked with Ag NPs, showed a transformation to Ag_2S while some of the Ag NPs detected in the effluent were still in the pristine metallic form[14]. Even though most NPs present in the natural environment are likely to have undergone some form of physicochemical transformation, very few effects studies have employed transformed NPs[15–17] or NPs in environmentally relevant media such as wastewaters[12,18,19]. One recent study has shown that Cu NP transformation through a septic tank led to a lack of toxicity in a zebrafish embryo hatching assay[15]. A decreased toxicity was also observed for the freshwater amphipod *H. Azteca* exposed to Ag NPs transformed through an

activated sludge simulation system[17] while another study showed an increased zebrafish embryo toxicity in the effluent of a similar system dosed with 4-16 mg/L Ag NPs[20]. Studies using sulfidized Ag NPs through wastewater treatment processes demonstrated that although Ag_2S NPs are less soluble, they can still be bioavailable to different organisms[21,22] and induce toxicity, though at lower levels compared to pristine Ag NPs[23]. This highlights the need of a better understanding of the behavior of NPs, their transformation and their toxicity in complex media.

It remains a challenging task to detect and quantify NPs at low, but environmentally relevant concentrations (< μg/L) in complex matrices such as wastewater, effluent, sewage sludge, and surface waters[24]. As a result, most environmental fate studies and toxicological assessments are conducted at much higher concentrations than those expected to be found in the environment[20], and studies taking into account relevant exposures at more realistic conditions are scarce[15,16]. There is a need to develop a better understanding of the environmental impact of transformed NPs at environmentally relevant concentrations[25].

The current study investigates the potential hazard of transformed Ag and TiO_2 NPs through advanced biological treatment processes present in complex environmental media such as WWTP effluents at environmentally relevant NP concentrations. A lab-scale pre-denitrifying WWTP system with pre-conditioned activated sludge was established and continuously fed with artificial wastewater dosed with 10 μg/L Ag and 100 μg/L TiO_2 NPs for a period of 5 weeks. The system was combined with a battery of marine and freshwater bioassays and NP characterization techniques to evaluate the hazard potential of transformed Ag and TiO_2 NPs. Sequential filtration combined with ICP-MS was applied to characterize the different size fractions (associated with settling solids, colloidal matter, nanoscale and dissolved). Both marine (*Skeletonema pseudocostatum*, *Tisbe battagliai*) and freshwater (*Raphidocelis subcapitata*,

Daphnia magna) organisms (algae and crustaceans) were used as model species to monitor the toxicity of the transformed NPs present in the effluent during the 5-week dosing period. The choice of organisms reflects that the behavior of NPs differs in marine and freshwater environments, the effects may vary depending on the species used[26] as well as the fact that in many countries the effluent is discharged in both freshwater and marine environments. Furthermore, an *in vitro* model using the rainbow trout (*Oncorhynchus mykiss*) gill cell line RTgill-W1 was employed, representing a major interface between the organism and its environment that is one of the first sites impacted by waterborne chemicals. The model was used in addition to the standard bioassays for assessment of the effluent with minimal sample modification during the period of dosing of the WWTP system and cellular responses were assessed (metabolic activity, epithelial integrity, reactive oxygen species (ROS) formation and the gene expression of zonula occludens-1 and multixenobiotic resistance genes ABCB1, ABCC1 and ABCC2).

MATERIALS AND METHODS

Nanoparticles and chemicals. Polyvinylpyrrolidone (PVP)-coated Ag NPs (Econix 25 nm, aqueous suspension) were obtained from Nanocomposix (Czech Republic). TiO_2 NPs (NM-101, primary particles of 5 nm) were obtained from the Joint Research Centre (JRC Repository, Ispra, Italy) and have been extensively characterized previously[27]. A stock dispersion of TiO_2 NPs in 0.22 µm filtered MilliQ (2.56 mg/ml) was prepared in a Scint-Burk glass vial and sonicated in ice water for 13 min with a calibrated probe sonicator according to the FP7 EU NANoREG sonication protocol[28]. The NP stock dispersions were then analyzed with scanning transmission

99 electron microscopy (STEM), single particle (sp-ICP-MS, see sections below) and dynamic light
100 scattering (DLS) (Supporting Information; SI). $AgNO_3$ (Sigma-Aldrich) was used as an ionic
101 control.

102 **Lab-scale wastewater treatment plant.** The lab-scale WWTP was a pre-denitrifying activated
103 sludge treatment system comprised of a 6.5 L non-aerated denitrifying reactor, an 8 L aerated
104 nitrifying reactor with automatic temperature (20°C) and pH (7.2) control and a 5.1 L settler (SI;
105 Figure S1). The activated sludge used in the system was collected from Bekkelaget WWTP,
106 Oslo, Norway. To adapt the activated sludge to the synthetic medium and to wash out any NPs
107 transferred to the system together with the initial sludge, the system was continuously fed
108 (hydraulic retention time ~15 h) synthetic wastewater without NPs for a period of 10 weeks. The
109 composition and characteristics of the synthetic wastewater and a detailed description of the
110 system operation and the parameters measured are presented in the SI. Sludge was continuously
111 removed from the denitrifying reactor to maintain a solids retention time (SRT) of ~15 days.
112 During the adaptation period effluent samples from the reference system without NPs were
113 collected weekly and served as "background controls". After the adaptation period the synthetic
114 medium was dosed with a continuous supply of 10 µg/L Ag NPs and 100 µg/L TiO_2 NPs to the
115 denitrifying reactor for a period of 5 weeks. The synthetic wastewater containing Ag and TiO_2
116 NPs was freshly prepared every 2-3 days. Effluent samples were collected weekly and used to
117 evaluate the influence of NP transformation on the battery of bioassays (performed within 48 h
118 of effluent collection). The COD and total inorganic N removal was 81±8 % and 71±16 %,
119 respectively (SI).

120 **Ag and TiO_2 NP characterization (STEM/EDS, sp-ICP-MS).** Ag, TiO_2 NP stock dispersions
121 or effluent samples were imaged using STEM, while elemental point analysis and mapping were

122 performed with energy-dispersive X-ray spectroscopy (EDS). A detailed description of the
123 STEM-EDS method is presented in the SI.

124 The effluent samples as prepared for STEM were transferred to Eppendorf tubes, vortexed for 30
125 s, sonicated for 30 min, and then diluted with MilliQ water prior to single particle ICP-MS (sp-
126 ICP-MS) analysis for particle concentration and size. The sp-ICP-MS analytical protocol and
127 data analysis (using the single particle RIKILT calculation tool[29], Wageningen, The Netherlands)
128 are similar to those described elsewhere[9,29] (detailed description of the sp-ICP-MS method in SI).

129 **Ag and TiO_2 fractionation (filtration, ultrafiltration and ICP-MS).** Samples from the
130 influent, nitrifying and denitrifying reactors, as well as the effluent (collected from the overflow
131 of the settler), were collected weekly and fractionated using a series of membranes with
132 decreasing pore size immediately upon sample collection. The samples were filtered sequentially
133 through a 0.7 μm filter membrane (glass microfiber GF/F, Whatman, GE Healthcare Life
134 Sciences), a 0.1 μm membrane (Durapore membrane filter, Millipore) and finally centrifuged
135 through a 3 kDa cut-off membrane (Amicon Ultra-15, Millipore, 5000g for 1 h) to obtain the
136 soluble fraction present in the filtrate sample. The 0.7 μm filters were dried at 45°C for 2 h and
137 kept in microwave tubes until further analysis (solid-associated fraction or particles >0.7 μm).
138 The solids-associated (>0.7 μm), particulate (0.1-0.7 μm), NP (3 kDa cut-off - 0.1 μm) and the
139 soluble fraction (3 kDa filtrate) were analyzed by ICP-MS (see SI for details).

140 ***Skeletonema pseudocostatum* growth inhibition assay.** The marine algae were cultured in ISO
141 media[30] prepared from filtered natural seawater (35 ppt salinity), and maintained at 20°C under
142 continuous light and shaking according to the ISO 10253 standard. Dilution water used for the
143 exposure assays was a modified version of the ISO media with a reduced concentration (1/5) of

144 trace elements and EDTA to minimize free metal ion complexation[31] and possible impacts on the
145 toxicity profile of the effluent. The effluent was spiked with concentrated ISO media stock
146 solutions to reach the elemental concentrations present in the dilution water. Artificial sea salts
147 (Coral Pro Salt) were added to reach 35 ppt salinity. Increasing concentrations (5 concentrations:
148 6.2-100%) of effluent or pristine NPs and $AgNO_3$ were placed in a 12-well plate (1.35 ml/well,
149 triplicates). Exponentially growing algae were counted with a hemocytometer and 150 µl of
150 $1 \cdot 10^5$ cells/ ml were added to each well (final algal concentration $1 \cdot 10^4$ cells/ml). An artificial
151 seawater control was prepared by spiking artificial sea salts (to achieve 35ppt) into clean dilution
152 water. Filtered natural seawater with reduced trace elements and EDTA concentrations served as
153 an untreated control while "background" effluent control was also included. The algal cell
154 density and growth was assessed daily for 72 h by measuring fluorescence (excitation 530 nm:
155 emission 685 nm, Victor^3 Multilabel plate reader, PerkinElmer). The specific growth rate
156 (logarithmic increase in biomass) and the percent growth inhibition over the exposure period was
157 calculated according to the ISO standard.

158 ***Raphidocelis subcapitata* growth inhibition assay.** The freshwater algae were cultured in EPA
159 media[32] and maintained at 20°C under continuous light and shaking according to the OECD 201
160 guideline. The effluent was spiked with concentrated nutrient stock solutions to achieve the same
161 concentration as the standard media. Trace elements and EDTA were used at a reduced
162 concentration (1/5). 1.35 ml of increasing concentrations of effluent (5 concentrations: 6.2-
163 100%), pristine NPs or $AgNO_3$ were placed in a 12-well plate. Finally, 150 µl of algae ($5 \cdot 10^5$
164 cells/ml) in exponential growing phase were added per well (final algae concentration $5 \cdot 10^4$
165 cells/ml). Dilution water (MilliQ water supplemented with the concentrated stock solutions and
166 1/5 trace elements-EDTA) served as an untreated control and effluent collected during the

stabilization period served as a "background" effluent control. The algal cell number and growth was measured daily for 72 h (fluorescence measurement, excitation 485 nm: emission 685 nm, Victor^3 Multilabel plate reader, PerkinElmer).

Effects of effluent on ROS formation (marine and freshwater algae). Exponentially growing algae were centrifuged and re-suspended in dilution water to achieve a concentration of $4 \cdot 10^6$ cells/ml. 25 µl of cell suspension was placed in each well of a 96-well plate (final algal concentration $1 \cdot 10^6$ cells/ml) and incubated in the dark with 25 µl DCFH-DA 20 µM (final concentration 10 µM) for 1.5 h under shaking conditions. At the end of the incubation period, 150 µl of effluent (serially diluted in dilution water) was added to each well and incubated for 1 h. At the end of the exposure period, DCF fluorescence was measured at wavelengths of 485 nm excitation and 535 nm emission. H_2O_2 was used as a positive control.

***Daphnia magna* acute toxicity assay.** Daphnids were maintained in M7 media[33] and fed with *R. subcapitata* every other day. Daphnids <24 h old were used for the assay, which was performed in 6-well plates as previously described[34] and according to OECD 202 guideline. Five daphnids per well were used in quadruplicate and were exposed to increasing concentrations of effluent (5 concentrations: 6.25-100%). Moderately hard EPA water was used for dilutions of the effluent[35]. Daphnids in EPA water served as an untreated control while exposure to effluent collected during the stabilization period served as a "background" effluent control. The effects of pristine Ag NPs as well as spiked in background effluent (0.005-0.32 mg/L) were also evaluated. Daphnid mobility was assessed after 24 and 48 h.

***Tisbe battagliai* acute toxicity assay.** *T. battagliai* were maintained in filtered (0.22 µm) seawater obtained from the outer Oslofjord and fed a mixed diet of *Rhodomonas baltica* and

189 *Isochrysis galbana.* Copepods of 6 ± 2 days old were used for the assay as previously
190 described[36]. Tests were performed in 12-well plates with 5 animals (4 replicates per treatment) in
191 each well containing ~4 ml of test solution. Artificial salts (Coral Pro Salt) were added to the
192 effluent to reach a salinity of 35 ppt, with further dilutions made in the natural seawater used for
193 culture maintenance. The effects of increasing concentrations of the effluent (5 concentrations:
194 6.25-100%), Ag NPs (0.08-1.3 mg/L), TiO_2 NPs (0.01-10 mg/L) or $AgNO_3$ (0.01-0.16 mg/L) in
195 seawater or spiked in background effluent were assessed after 24 and 48 h of exposure. MilliQ
196 water spiked with artificial sea salts acted as an artificial seawater control. Natural seawater
197 served as an untreated control.

198 **RTgill-W1 *in vitro* model in transwell inserts.** The rainbow trout gill epithelial cell line RTgill-
199 W1[37] was provided by Prof. Kristin Schirmer (EAWAG, Switzerland). Cells were cultured in
200 Leibovitz's L-15 medium (L-15, Gibco, ThermoFischer Scientific) supplemented with 5% fetal
201 bovine serum (FBS, Gibco, ThermoFischer Scientific) and 1% gentamicin solution (10 mg/ml,
202 Sigma-Aldrich), and maintained at 19 °C in an incubator in the absence of CO_2. The cells were
203 seeded in 12-well transwell inserts (Millicell Hanging Cell Culture Insert, 1.0 µm, Merck
204 Millipore) at a concentration of $1.8 \cdot 10^5$ cells/ml (0.5 ml cell suspension/insert). The basolateral
205 compartment was filled with 1.5 ml of complete L-15 cell culture medium in a 12-well receiver
206 plate (Merck Millipore). Cells were allowed to grow for 10 days and form a confluent
207 monolayer. The media was renewed every other day.

208 **Metabolic activity and epithelial integrity.** On day 10, the cells were exposed for 24 h to
209 increasing concentrations of the freshly collected effluent from the system (filtered through a 0.2
210 µm filter; serial dilutions with a dilution factor of 2), the pristine NPs or $AgNO_3$. Dilutions were
211 performed in L15/ex media as previously described[37,38]. Cells in L15/ex media served as an

212 untreated control. At the end of the exposure period the media was removed and replaced with
213 L15/ex media containing 100 µM alamar blue solution. Cells were incubated for 1 h and
214 fluorescence was measured at wavelengths of 530 nm excitation and 590 nm emission (Victor^3
215 Multilabel plate reader, PerkinElmer). The alamar blue solution was then removed and replaced
216 with 0.1 mg/ml lucifer yellow (LY, Sigma-Aldrich) solution as a marker for paracellular
217 permeability. The cells were incubated for 2 h before the inserts were removed from the receiver
218 plates and fluorescence was measured at wavelengths of 485 nm excitation and 535 nm emission
219 (Victor^3 Multilabel plate reader, PerkinElmer).

220 **Quantitative real time PCR (qPCR).** After exposure of the RTgill-W1 cells in transwell
221 inserts, the exposure medium was removed, the cells were washed in PBS and were collected
222 with 300 µl RLT plus buffer (Qiagen) supplemented with 1% mercaptoethanol. Total RNA was
223 extracted using RNeasy Plus Mini Kit (Qiagen) according to the manufacturer´s instructions and
224 as previously described[39]. The RNA purity and concentration were determined using a Nanodrop
225 ND1000 spectrophotometer while RNA integrity was determined with an Agilent Bioanalyzer
226 RNA 6000 nano series kit (Agilent technologies, USA). The qPCR was performed as previously
227 described[39] (protocol details can be found in SI).

228 **Effects of effluent on ROS formation (*in vitro*).** RTgill-W1 cells were seeded in 96-well plates
229 at a concentration of $5 \cdot 10^5$ cells/ml (100 µl cell suspension/well). After 24 h, the media was
230 removed and fresh media containing 25 µM DCFH-DA in L15/ex media was placed in each well
231 (100 µl solution/well). After a 1 h incubation, the DCFH-DA solution was removed and replaced
232 with increasing concentrations of effluent (5 concentrations: 6-100%), Ag NPs, TiO_2 NPs or
233 $AgNO_3$ diluted in L15/ex. Fluorescence was measured after 1 and 2 h of exposure at wavelengths
234 of 485 nm excitation and 535 nm emission. H_2O_2 was used as a positive control.

Statistical analysis. Statistical analysis was performed with GraphPad Prism 6 (GraphPad Software, La Jolla, CA 92037, USA). Values are expressed as means ± standard deviation. Significant differences between the different treatments and control were analyzed with one-way analysis of variance (ANOVA) followed by Dunnet´s multiple comparison test or nonparametric Kruskal-Wallis test followed by Dunn's multiple comparison test. Statistical significance was defined at $p<0.05$. Dose-response curves, EC_{10} and EC_{50} values were obtained with GraphPad Prism 6 (GraphPad Software, La Jolla, CA 92037, USA) using a logistic four-parameter model. Principal component analysis (PCA) of the parameters and effects observed with the different bioassays was performed with XLSTAT 2018 (SI).

RESULTS AND DISCUSSION

Ag and TiO_2 Nanoparticle characterization. The physicochemical properties determined for the Ag and TiO_2 NP stock dispersions in MilliQ water are summarized in the SI (Figures S2-3, Table S1). The Ag NPs were spherical with a mean diameter of 26.5 ± 0.7 nm and 58.8 ± 0.19 nm according to sp-ICP-MS and DLS measurements, respectively. DLS and sp-ICP-MS analyses showed an average TiO_2 aggregate size of 640.7 ± 9.2 and 278 ± 15 nm, respectively. STEM imaging indicated that TiO_2 NPs were porous and formed large aggregates consisting of individual particles below 10 nm, confirming previous reports on this material[27]. In synthetic wastewater and seawater TiO_2 aggregates of 969 ± 19 nm and 1375 ± 76.7 nm, respectively were measured with DLS (SI; Table S1). Ag NPs in synthetic wastewater, seawater and the exposure media used in the bioassays ranged from 57.3 ± 0.17 to 59.5 ± 0.18 nm as measured with DLS, suggesting a stability of the PVP-coated Ag NPs in the different media. The higher (~2x) particle size obtained for both pristine Ag NPs and TiO_2 with DLS is probably related to the inherent properties of the instrument, light scattering techniques such as DLS require higher

concentrations that can result in aggregation that could influence the analytical signal[40]. With sp-ICP-MS low concentration levels can be detected in more complex or natural environmental samples. Therefore, multiple analytical techniques are necessary especially for low NP concentrations in environmental samples.

Ag and TiO_2 NP transformation in the lab-scale WWTP. Sequential filtration and ICP-MS analysis of the individual effluent fractions showed that >80% of the Ag and Ti measured was associated with suspended solids (>0.7 μm fraction) present in the effluent samples (Figure 1, Figure S4). The highest concentrations of both total Ag and Ti were observed in effluents from weeks 2 and 5. The Ti levels in the fraction >0.7 μm ranged from 0.9-24.2 μg/L, with the highest concentration measured at week 2. The dissolved Ag concentration was in the range of 0.005-0.021 μg/L (Table 1). The highest dissolved Ag concentrations were observed in effluents collected after 1 and 3 weeks of NP dosing, and corresponded to 7-8% of the total Ag measured during those weeks. The Ag concentration present in the NP fraction ranged from 0.1-0.22 μg/L, with the highest concentrations measured in the effluent samples collected in weeks 1, 3 and 5 (0.22, 0.14 and 0.17 μg/L, respectively). The Ti present in the 0.1 μm and 3 KDa fractions could not be distinguished and quantified separately, therefore the values are reported as Ti >0.7 μm and <0.7 μm. A previous study with sequencing batch reactors showed that a significant fraction of Ag was associated with colloidal material (below 0.45 μm)[41] and biosolids in the sludge and effluent of a pilot WWTP[14].

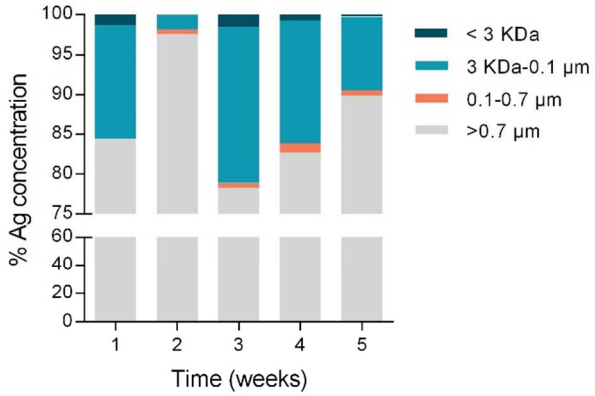

Figure 1. Effluent characterization and distribution of the total Ag present in the effluent of the lab-scale WWTP system during the 5 weeks of continuous dosing of the system.

Table 1. Ag and Ti concentrations (µg/L or µg/g effluent suspended solids) in each effluent fraction during the 5 weeks of operation and continuous dosing of the lab-scale WWTP system.

	Ag concentration								Ti concentration			
	Total		>0.7 µm		nano-Ag		3 KDa filtrate		>0.7 µm		<0.7µm	
Effluent Sample	µg/L	µgAg/gSS	µg/L	µgAg/gSS	µg/L	µgAg/gSS	µg/L	µgAg/gSS	µg/L	µgTi/gSS	µg/L	µgTi/gSS
wk 1	0.74	47.34	0.51	32.21	0.22	13.82	0.02	1.31	0.90	57.50	0.14	8.67
wk 2	5.99	72.15	5.84	70.41	0.11	1.28	<0.005	0.06	24.20	291.52	0.13	1.55
wk 3	0.72	66.28	0.56	51.88	0.14	12.98	0.01	1.01	1.00	92.17	0.16	14.81
wk 4	0.65	47.90	0.54	39.60	0.10	7.37	<0.005	0.37	2.50	183.15	0.10	7.50
wk 5	1.80	333.22	1.62	299.75	0.17	30.59	<0.005	0.93	5.40	999.30	0.15	27.04

The effluent collected during the 4th week of system operation was analyzed by STEM in combination with EDS to determine both the presence and transformation of Ag and TiO_2 NPs. Electron microscopy images showed the presence of particles with high mass (bright contrast), while EDS analysis indicated that Ag-rich particles were associated with S, Cu and Zn (Figure 2A). STEM also showed the presence of TiO_2 polycrystalline aggregates (~50 nm) (Figure 2B)

290 comprised of primary particles below 10 nm which were similar to the initially dosed particles.
291 The association of Ag present in WWTP with elements such as Cu, Zn and S is in accordance
292 with previous studies reporting the presence of Ag particles associated with S in sludge[14,42] and
293 effluent samples[14]. It has recently been shown that secondary nano-sized Ag particles of
294 approximately 20 nm diameter associated with S from organic or inorganic source are formed
295 from dissolved silver from Ag NPs (80 nm, PVP coated) in batch systems with wastewater
296 effluent and mixed liquor[10].

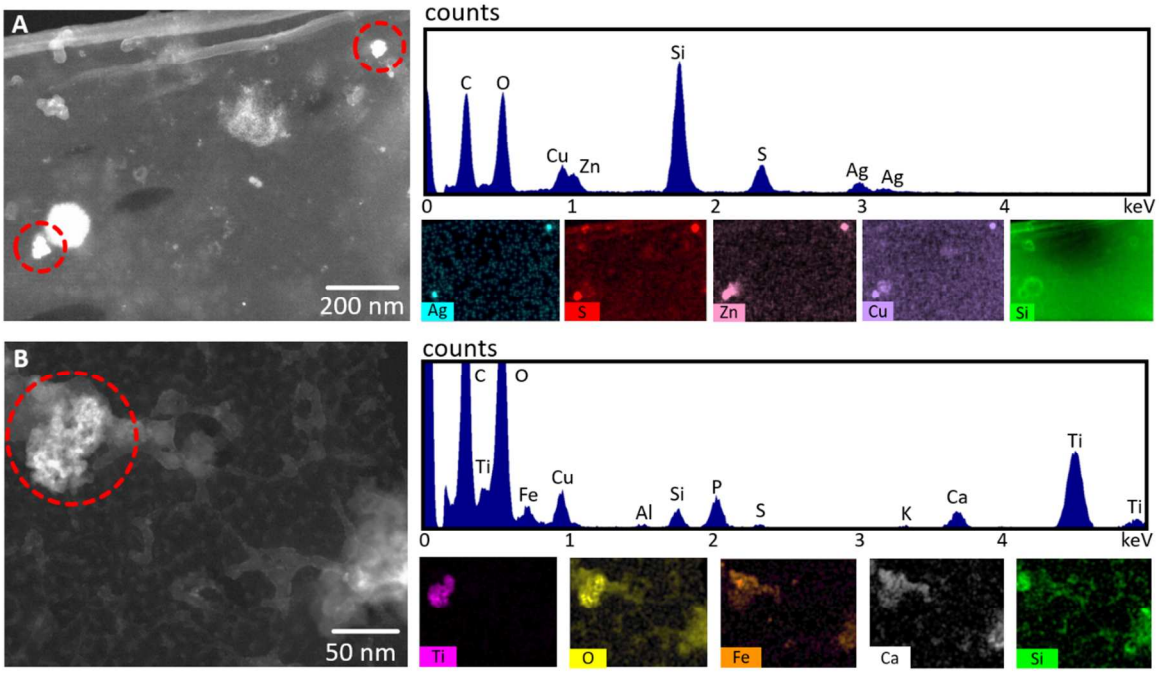

297

298 **Figure 2.** STEM images of (A) Ag-rich and (B) TiO_2 particles from the lab-scale WWTP,
299 together with sum spectra of the encircled regions and elemental maps. Particles were detected in
300 the effluent collected during the 4th week of dosing and operation of the system.

301

Single particle ICP-MS analysis of effluent samples collected during the 5 weeks of operation of the system confirmed the presence of Ag and TiO_2 NPs, indicating they occurred within the size ranges 20.5-31.6 nm and 110.9-124.8 nm, respectively (SI; Table S1). Sp-ICP-MS is a very promising technique for the identification and quantification of metallic NPs in complex matrices[43], including wastewater and effluents[44–46]. The technique has low detection limits[47] and requires highly diluted samples that are very relevant for environmental samples, as well as when realistic exposures are to be studied. However, distinction between Ag complexes and species or Ag bound colloids cannot be made[45].

Effects of effluents on algal growth and ROS formation. A 20-40% growth inhibition of the marine algae, *S. pseudocostatum,* was observed upon exposure to effluents at the highest effluent concentration (100%; Ag and Ti exposure concentrations of 6 and 24 µg/L, respectively), with effluent from week 2 showing the strongest effect (40% growth inhibition relative to untreated control) (Figure 3). However, results from the DCFH-DA assay indicated that no formation of ROS occured for any of the tested effluents (SI; Figure S5). Exposure to the background effluent alone did not result in any significant effect on algal growth. These concentrations are below the respective no effect concentration (NOEC) values obtained for *S. pseudocostatum* in this study (1 mg/L and 10 mg/L for Ag and TiO_2 NPs). This suggests that the presence of solids and elevated NH_4 concentrations (3.3 mg/L) contribute to the observed effects and not just the total Ag and Ti present in the effluents (Table S2, Figure S8). Differences in toxicity of Ag NPs aged in crude and final wastewater have been reported and decreased toxicity was related to the sample physicochemical parameters and increased complexity[48].

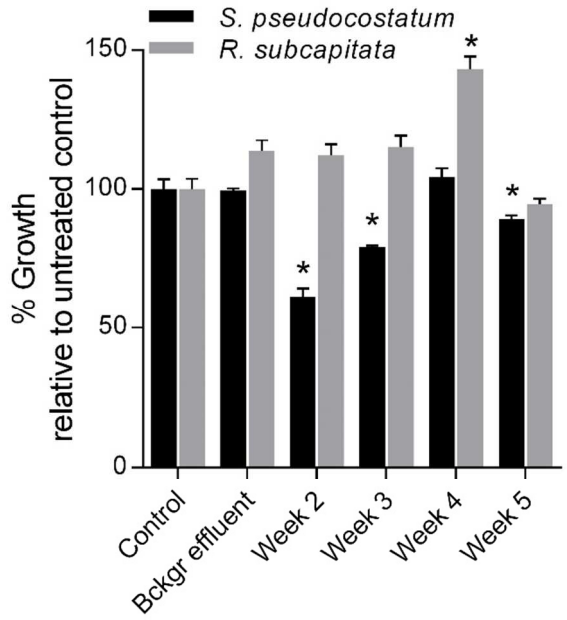

323

324 **Figure 3**. Percentage growth of *S. pseudocostatum* (black bars) and *R. subcapitata* (grey bars)
325 exposed to effluents collected in weeks 2-5 (100% and 50% effluent concentration for *S.*
326 *pseudocostatum* and *R. subcapitata*, respectively) and the background effluent. Algal growth
327 inhibition was determined after 72 h of exposure. Asterisks denote statistical significance at
328 $p<0.05$.

329

330 In contrast to the inhibitory effects of the effluent on *S. pseudocostatum* growth, there was
331 evidence of hormetic effects in the freshwater algae, *R. subcapitata* exposed to effluent
332 concentrations <50%. These effects were most apparent after exposure to effluent collected from
333 week 4 and showed significant stimulatory effects on growth compared to the control (40%
334 increase in growth compared to control) (Figure 3). The stimulatory effects in *R. subcapitata*
335 growth were accompanied by a significant increase in the ROS formation (1.6-1.9-fold compared
336 to untreated control) (SI; Figure S5) and increased cell aggregation (observed by microscopy,

337 data not shown). The ROS formation was positively correlated with the total Ag and Ti
338 concentration, total N and suspended solids present in the effluents (Figure S8). A similar
339 response of cell aggregation has been previously reported upon exposure of the green algae
340 *Chlamydomonas reinhardtii* to CuO-polystyrene core-shell NPs[49] and *Chlorella vulgaris* and
341 *Dunaliella tertiolecta* to Ag NPs[50]. It has been suggested that cell aggregation is a defense
342 mechanism that decreases the amount of exposed surface to xenobiotics. Moderate stress and low
343 ROS levels can lead to hormetic effects that can in turn induce the defense system[51]. The results
344 from the current study indicate that responses to the effluent exposure are species-dependent,
345 possibly due to differences in cell size, surface area and cell wall composition. Studies with
346 green algae and cyanobacteria exposed to Ag NPs have also shown differences in cell viability
347 and ROS response between species attributed to different biological properties and the
348 production of extracellular polymeric substances[52]. Moreover, the NP behavior depends on the
349 media composition that can result in different responses, TiO_2 aggregates of 1369 nm were
350 observed in the presence of Cl in the higher ionic strength media of *S. pseudocostatum* compared
351 to 650 nm aggregates in *R. subcapitata* media while the Ag NPs seemed to be stable in both
352 media. The formation of insoluble AgCl(s) and dissolved silver chloride species depends on the
353 Cl/Ag ratio[53] which could further explain differences in effects observed between the freshwater
354 and marine algae.

355 **Effects of effluents on *T. battagliai* and *D. magna*.** Exposure to effluents collected weekly
356 during the operation of the system led to a 20-45% increase in mortality of *T. battagliai* (at 100%
357 effluent concentration), while no effect was observed from the background effluent (Figure 4A).
358 The highest significant mortality was observed upon exposure to effluents collected in weeks 2
359 and 5 (35 and 45% mortality compared to untreated control, respectively). Spiking the

360 background effluent with increasing concentrations of Ag NPs elicited a reduction in toxicity at
361 the lowest Ag NP concentration (0.08 mg/L) compared to pristine Ag NPs, but still caused a
362 significant increase in mortality at most concentrations (Figure 4B). Spiking the background
363 effluent also resulted in a 1.9x increase in the EC_{50} value compared to the pristine Ag NPs (0.09
364 and 0.17 mg/L, respectively) although the EC50 values were not statistically significant (Figure
365 4B). TiO_2 NPs did not have any effect on mortality at any of the concentrations tested (0.01-10
366 mg/L).

367 Although the total Ag concentration in the effluents (5.99 µg/L or 72.15 µg/gSS) exceeded the
368 NOEC for Ag NPs (0.005 mg/L), and was at a similar level to the EC_{10} obtained in this study
369 (0.0076 mg/L), no adverse effects on daphnid mobility were observed following 48 h exposure to
370 either the effluents or the background effluent. Spiking of the background effluent with
371 increasing concentrations of Ag NPs led to a significant decrease in mobility, but resulted in an
372 16x increase in the EC_{50} value compared to the pristine Ag NPs (0.16 and 0.0098 mg/L,
373 respectively) (Figure 5). TiO_2 NPs did not affect daphnid mobility.

374

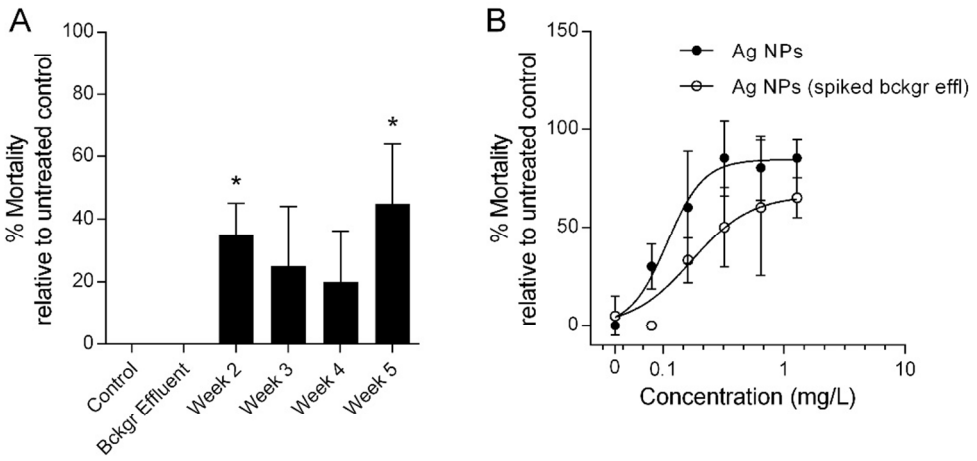

375

376 **Figure 4**. Percentage mortality of *T. battagliai* following 48 h exposure to (A) effluents collected
377 in weeks 2-5 and (B) increasing Ag NP concentrations as received or spiked in the background
378 effluent. Asterisks denote statistical significance at $p<0.05$.

379

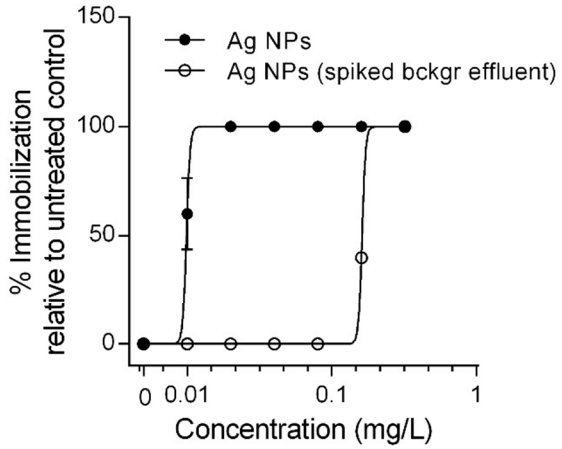

380

381 **Figure 5.** Percentage immobilization of *D. magna* juveniles following 48 h exposure to
382 increasing Ag NP concentrations and Ag NP-spiked background effluent. Background effluent
383 was collected during the system stabilization period (prior to spiking). No effects of effluents
384 collected in weeks 2-5 and background effluent were observed.

385

386 A clear reduction in the toxicity of Ag NPs to *D. magna* was observed when exposed to the
387 effluent collected from the lab-scale WWTP system (containing transformed Ag NPs) compared
388 to pristine Ag NPs. Unlike *D. magna*, the marine copepod *T. battagliai* exhibited a clear
389 response following exposure to the week 2-5 effluents (statistically significant in weeks 2 and 5).
390 The difference in response between the two species may result from a combination of NP
391 behavior in more complex WWTP effluents and differences in the feeding behavior of the two
392 organisms. *D. magna* is a planktonic filter feeding organism[54] while *T. battagliai* is an
393 opportunistic feeding epibenthic organism[55]. Therefore, *T. battagliai* is likely to be directly in
394 contact with particles associated with effluent solids that may settle out during the exposure
395 period. *T. battalgiai* are non-selective grazers as well as filter feeders and feed on suspended
396 particles along with detritus that settles out of the water column[56]. These differences in feeding
397 habit could explain the increased sensitivity of the copepods compared to daphnids when
398 exposed to the WWTP effluent. In contrast to this *D. magna* was 10x more sensitive to pristine
399 Ag NPs compared to *T. battagliai* (Figure 4 and 5). Therefore, the complete absence of effects in
400 *D. magna* exposed to any of the collected effluents reinforces the idea that NPs present in the
401 effluent are associated with the solids settling on the bottom of the vessels, reducing direct
402 exposure and ingestion by the daphnids.

403 To further confirm this, *T. battagliai* and *D. magna* were exposed to the background effluent
404 spiked with increasing concentrations of Ag NPs which led to decreased toxicity relative to the
405 pristine Ag NPs. However, for *T. battagliai* the EC_{50} value only increased 2 times, whereas for
406 *D. magna* the EC_{50} value increased 16 times. This indicates the presence of solids in the effluent,
407 as well as the potential formation of precipitates, reduces the bioavailability of the Ag NPs to the

daphnids compared to *T. battagliai*. This is in accordance with previous studies where reduced toxicity of $AgNO_3$ spiked into untreated effluent was observed for the freshwater green algae *C. reinhardtii*[19] and the protective effects of background effluent were observed towards Cu interference with zebrafish hatching[15]. Furthermore, a decrease in the bioavailability of Ag from $AgNO_3$-exposed algae (*C. reinhardtii*) was observed in wastewaters, and suggested to be due to the presence of ligands[12]. It has been previously demonstrated that sulfidation[53], the presence of natural organic matter[57] and thiol- or selenide-containing compounds such as cysteine[58] can reduce the Ag NP dissolution rate and lead to protective effects due to Ag^+ complexation and decreased bioavailability[59,60], partially explaining the reduced toxicity of Ag NPs spiked in background effluent. The differences in EC50 increase trends of Ag NP-spiked background effluent compared to pristine Ag NPs between the 2 organisms can also be attributed to differences in media composition and ionic strength. The formation of AgCl precipitates in media with high Cl content such as in seawater can further impact the Ag^+ availability and subsequent toxicity[53,61]. Species-specific differences were related to the degree of Ag NP sulfidation, the exposure route and species sensitivity[53].

Therefore, the effects of Ag NPs observed in the current study are considered organism-dependent, with (epi)benthic organisms having the highest exposure risk due to directly ingesting sedimented and aggregated NPs or NPs bound to effluent solids. In addition, the media composition can impact the NP speciation and behavior leading to increased TiO_2 NP aggregation and formation of silver chloride species in media of increasing ionic strength.

Effects of effluents on RTgill-W1 cells. The *in vitro* fish gill cell line model was employed in the current study as the gill is a key site for xenobiotic uptake and it is continuously exposed to water-borne contaminants[62]. Furthermore, the gills express enzymes involved in xenobiotic

431 metabolism and transport. Exposure to the 1-5 week effluents did not cause a statistically
432 significant decrease in the metabolic activity of RTgill-W1 cells in transwell inserts (Figure 6). A
433 40% decrease in the epithelial integrity (Figure 6), which coincided with a 2-fold increase in
434 ROS formation (Figure S6), was observed upon exposure to effluent from week 3. However, no
435 statistically significant effect was observed for any of the other effluents and no effect was
436 observed for the "background" effluent for either endpoint. Previous studies have shown that
437 primary fish gill cell cultures in permeable filter supports can tolerate apical water and varying
438 osmotic conditions[63], river water[64], detect bioreactive metals[64,65], and have been used to study the
439 uptake and transport of Ag NPs[66]. In the current study, it has proven to be a good model system
440 for whole effluent toxicity testing without the need for sample modification or alteration of the
441 water chemistry prior to exposure. However, the concentrations of Ag and TiO_2 NPs measured in
442 the effluent are considered too low to fully account for the effects observed in the metabolic
443 activity and epithelial integrity assays. Given the complexity of the wastewater effluent, it
444 appears that the combination of the presence of Ag NPs, ionic Ag and additional stressors such
445 as NO_3 contribute to the overall response observed (Figure S8).

446

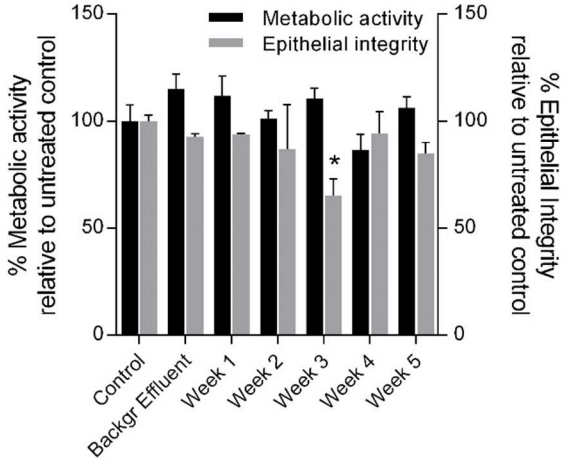

Figure 6. Percentage change in metabolic activity (left Y axis, black bars) and epithelial integrity (right Y axis, grey bars) of RTgill-W1 cells following exposure to effluents collected in weeks 1-5. Asterisks denote statistical significance at $p<0.05$.

As effects were observed on the epithelial integrity, and because the gill is a site of xenobiotic uptake and detoxification, the effects of the effluents on the gene expression of zonula occludens-1 (ZO-1) tight junction protein and multixenobiotic resistance genes in RTgill-W1 cells were studied. The ZO-1 gene was selected due to the decreased epithelial integrity observed in the paracellular permeability assay. Results showed ZO-1 mRNA levels were elevated after exposure to effluents collected on week 1 and 3 (SI; Figure S7). Previous studies have shown that the RTgill-W1 cells express functional tight junctions that can respond to certain modulators[67]. In the current study, the RTgill-W1 cell model in transwell inserts showed an increased paracellular permeability followed by an increase in ZO-1 expression upon exposure to week 3 effluent, suggesting an impact on the epithelial integrity and a compromised barrier function. Moreover, the DCFH-DA assay indicated exposure to the week 3 effluent led to a 2-

fold increase in ROS formation, suggesting a ROS-induced compromised epithelial integrity. It has previously been shown that oxidative stress can lead to a disruption of tight junctions in MDCK canine kidney cells[68].

The multixenobiotic resistance (MXR) mechanism mediated by ATP binding cassette transporters is an important mechanism of defense against xenobiotics, which functions by extruding them or their metabolites out of the cell. The transporters are localized in tissues with a barrier function or involved in secretion and absorption, they transport a wide variety of compounds across cell membranes and it has recently been shown that NPs, including Ag NPs, can interfere with the MXR system[69,70]. Due to their importance in cellular defense against xenobiotics, the multixenobiotic resistance genes ABCB1, ABCC1, ABBC2 were also investigated in the current study. Exposure to the effluents led to increased mRNA levels of ABCB1, ABCC1 and ABCC2 transporters, with ABCB1 (the most responsive) exhibiting increased expression levels in response to effluents from weeks 1-3 (3.4-fold increase upon exposure to effluent week 2) (SI; Figure S7). These results indicate an interference with the defense mechanism and potentially compromised protection against xenobiotics. The contribution of other trace elements and other unidentified stressors present in the effluent to the observed effects cannot be excluded. It also remains to be determined whether this observed change in gene expression also leads to transporter functional changes.

Environmental implications. The combination of a lab-scale WWTP with detailed fractionation approaches, characterization techniques (TEM, sp-ICP-MS, sequential filtration/ICP-MS), a battery of marine and freshwater bioassays and an *in vitro* gill cell line model allowed the effects of transformed NPs to be investigated. This study shows that Ag NPs are transformed through simulated biological WWTP processes to particles associated with S, Cu and Zn. The resulting

hazard cannot be predicted based on exposures made in simplified media or determined by measuring the NP concentration and the dissolved fraction since the effluent is complex with additional stressors (e.g suspended solids, NH_4) either exacerbating or mitigating the effects depending on the organism, endpoint and media used. The transformed particles appeared to have a greater impact on epibentic copepods suggesting that they were still bioavailable despite their transformation. Differences in responses in marine vs freshwater algae and crustaceans highlight the importance of the media composition in the NP speciation that can lead to species-specific responses. The study reinforces the need to use multiple test species representing different environments and exposure routes, bioassays and endpoints to gain clearer understanding of the potential hazards of low level realistic concentrations of transformed nanomaterials and multiple stressors in environmental media of increased complexity. The results highlighting the difference in toxicity of pristine and transformed particles, emphasize the need for future studies using a broader range of weathered or transformed NPs in relevant exposure scenarios to provide a more accurate understanding of their potential impacts. The combination of complementary analytical techniques (TEM, sp-ICP-MS, sequential filtration/ICP-MS) was useful for the detection and characterization of low NPs concentrations in complex environmental matrices. Our results demonstrated that Ag and TiO_2 NPs show a strong association with solids, suggesting the potential for terrestrial organisms' exposure through biosolid[21,42,71] application. Based on these conclusions future studies should focus on the effects of transformed NPs associated with the biosolids on terrestrial organisms and the factors contributing to species-specific responses.

ASSOCIATED CONTENT

Supporting Information. Additional information is provided for the synthetic wastewater composition, the lab-scale WWTP description and operation (and schematic; Figure S1), sample preparation description for STEM/EDS and sp-ICP-MS, mass balance calculations for Ag and TiO_2 NPs, DLS measurements of TiO_2 and Ag NPs stock dispersions in MilliQ water, synthetic wastewater, seawater and exposure media, sp-ICP-MS measurements of NP stock dispersions and effluents (Table S1), characteristics of the effluents collected in weeks 1-5 (Table S2) and an overview of genes, primer sequences and protocol used for qPCR (Table S3). In addition, TEM images of Ag and TiO_2 NPs stock dispersions are provided (Figure S2, S3), fractionation of Ti (Figure S4), effects of effluents on *S. pseudocostatum* and *R. subcapitata* ROS formation (Figure S5), effects of effluents on RTgill-W1 ROS formation (Figure S6), gene expression (Figure S7) and principal component analysis (PCA) of the physicochemical parameters and effects observed in the different bioassays (Figure S8).

AUTHOR INFORMATION

Corresponding Author

* Anastasia Georgantzopoulou. E-mail: anastasia.georgantzopoulou@niva.no. Tel: +4798227741

Author Contributions

The manuscript was written through contributions of all authors. All authors have given approval to the final version of the manuscript.

ACKNOWLEDGMENT

The work reported here has been undertaken as part of the Research Council of Norway (RCN) funded project NanoWASTE "Investigating the fate of nanomaterials in waste water treatment plants; removal, release and subsequent impacts" (Grant Agreement number 238972/O70). The authors wish to thank the RCN for their financial support. This study also received support from the FORURENS Nanoparticle Characterisation in Environmental Media: Linking exposure to effects NANOCHARM (Researcher project - MILJØ2015). We would like to thank Pawel Krzeminski, Wolfgang Uhl and Adam Lillicrap (Norwegian Institute for Water Research, Oslo, Norway) for the useful insights and discussions. The authors gratefully acknowledge Maria Hultman (Norwegian Institute for Water Research, Oslo, Norway) for her valuable advice and help with the qPCR analysis and Marianne S. Kjos (SINTEF Materials and Chemistry) for the ICP-MS analysis. The authors would also like to acknowledge support from the Research Council of Norway through the Norwegian Center for Transmission Electron Microscopy, NORTEM (Grant Agreement number 197405/F50).

544 REFERENCES

545 (1) Weir, A.; Westerhoff, P.; Fabricius, L.; Hristovski, K.; Von Goetz, N. Titanium Dioxide
546 Nanoparticles in Food and Personal Care Products. *Environ. Sci. Technol.* **2012**, *46* (4),
547 2242–2250.

548 (2) Voelker, D.; Schlich, K.; Hohndorf, L.; Koch, W.; Kuehnen, U.; Polleichtner, C.; Kussatz,
549 C.; Hund-Rinke, K. Approach on Environmental Risk Assessment of Nanosilver Released
550 from Textiles. *Environ. Res.* **2015**, *140*, 661–672.

551 (3) Kiser, M. A.; Westerhoff, P.; Benn, T.; Wang, Y.; Pérez-Rivera, J.; Hristovski, K.
552 Titanium Nanomaterial Removal and Release from Wastewater Treatment Plants.
553 *Environ. Sci. Technol.* **2009**, *43* (17), 6757–6763.

554 (4) Li, L.; Hartmann, G.; Döblinger, M.; Schuster, M. Quantification of Nanoscale Silver
555 Particles Removal and Release from Municipal Wastewater Treatment Plants in Germany.
556 *Environ. Sci. Technol.* **2013**, *47*, 7317–7323.

557 (5) Johnson, A. C.; Jürgens, M. D.; Lawlor, A. J.; Cisowska, I.; Williams, R. J. Particulate
558 and Colloidal Silver in Sewage Effluent and Sludge Discharged from British Wastewater
559 Treatment Plants. *Chemosphere* **2014**, *112*, 49–55.

560 (6) Westerhoff, P.; Song, G.; Hristovski, K.; Kiser, M. A. Occurrence and Removal of
561 Titanium at Full Scale Wastewater Treatment Plants: Implications for TiO_2
562 Nanomaterials. *J. Environ. Monit.* **2011**, *13* (5), 1195.

563 (7) Polesel, F.; Farkas, J.; Kjos, M.; Almeida Carvalho, P.; Flores-Alsina, X.; Gernaey, K. V;

564 Foss Hansen, S.; Plosz, B. G.; Booth, A. M. Occurrence, Characterisation and Fate of
565 (Nano)Particulate Ti and Ag in Two Norwegian Wastewater Treatment Plants. *Water Res.*
566 **2018**, *141*, 19–31.

567 (8) Kaegi, R.; Voegelin, A.; Ort, C.; Sinnet, B.; Thalmann, B.; Krismer, J.; Hagendorfer, H.;
568 Elumelu, M.; Mueller, E. Fate and Transformation of Silver Nanoparticles in Urban
569 Wastewater Systems. *Water Res.* **2013**, *47* (12), 3866–3877.

570 (9) Li, L.; Stoiber, M.; Wimmer, A.; Xu, Z.; Lindenblatt, C.; Helmreich, B.; Schuster, M. To
571 What Extent Can Full-Scale Wastewater Treatment Plant Effluent Influence the
572 Occurrence of Silver-Based Nanoparticles in Surface Waters? *Environ. Sci. Technol.*
573 **2016**, *50* (12), 6327–6333.

574 (10) Azodi, M.; Sultan, Y.; Ghoshal, S. Dissolution Behavior of Silver Nanoparticles and
575 Formation of Secondary Silver Nanoparticles in Municipal Wastewater by Single-Particle
576 ICP-MS. *Environ. Sci. Technol.* **2016**, *50* (24), 13318–13327.

577 (11) Levard, C.; Hotze, E. M.; Lowry, G. V; Brown, G. E. Environmental Transformations of
578 Silver Nanoparticles: Impact on Stability and Toxicity. *Environ. Sci. Technol.* **2012**, *46*
579 (13), 6900–6914.

580 (12) Azimzada, A.; Tufenkji, N.; Wilkinson, K. J. Transformations of Silver Nanoparticles in
581 Wastewater Effluents: Links to Ag Bioavailability. *Environ. Sci. Nano* **2017**, *4*, 1339–
582 1349.

583 (13) Kent, R. D.; Oser, J. G.; Vikesland, P. J. Controlled Evaluation of Silver Nanoparticle
584 Sulfidation in a Full-Scale Wastewater Treatment Plant. *Environ. Sci. Technol.* **2014**, *48*

585 (15), 8564–8572.

586 (14) Kaegi, R.; Voegelin, A.; Sinnet, B.; Zuleeg, S.; Hagendorfer, H.; Burkhardt, M.; Siegrist,
587 H. Behavior of Metallic Silver Nanoparticles in a Pilot Wastewater Treatment Plant.
588 *Environ. Sci. Technol.* **2011**, *45* (9), 3902–3908.

589 (15) Lin, S.; Taylor, A. a.; Ji, Z.; Chang, C. H.; Kinsinger, N. M.; Ueng, W.; Walker, S. L.;
590 Nel, A. E. Understanding the Transformation, Speciation, and Hazard Potential of Copper
591 Particles in a Model Septic Tank System Using Zebrafish to Monitor the Effluent. *ACS*
592 *Nano* **2015**, *9* (2), 2038–2048.

593 (16) Holden, P. A.; Gardea-Torresdey, J. L.; Klaessig, F.; Turco, R. F.; Mortimer, M.; Hund-
594 Rinke, K.; Cohen Hubal, E. A.; Avery, D.; Barceló, D.; Behra, R.; Cohen, Y.; Deydier-
595 Stephan, L.; Ferguson, P. L.; Fernandes, T. F.; Herr Harthorn, B.; Henderson, W. M.;
596 Hoke, R. A.; Hristozov, D.; Johnston, J. M.; et al. Considerations of Environmentally
597 Relevant Test Conditions for Improved Evaluation of Ecological Hazards of Engineered
598 Nanomaterials. *Environ. Sci. Technol.* **2016**, *50* (12), 6124–6145.

599 (17) Kühr, S.; Schneider, S.; Meisterjahn, B.; Schlich, K.; Hund-Rinke, K.; Schlechtriem, C.
600 Silver Nanoparticles in Sewage Treatment Plant Effluents: Chronic Effects and
601 Accumulation of Silver in the Freshwater Amphipod *Hyalella Azteca*. *Environ. Sci. Eur.*
602 **2018**, *30* (1), 1–11.

603 (18) Bruneau, A.; Turcotte, P.; Pilote, M.; Gagné, F.; Gagnon, C. Fate of Silver Nanoparticles
604 in Wastewater and Immunotoxic Effects on Rainbow Trout. *Aquat. Toxicol.* **2016**, *174*,
605 70–81.

606 (19) Thalmann, B.; Voegelin, A.; Von Gunten, U.; Behra, R.; Morgenroth, E.; Kaegi, R. Effect
607 of Ozone Treatment on Nano-Sized Silver Sulfide in Wastewater Effluent. *Environ. Sci.*
608 *Technol.* **2015**, *49* (18), 10911–10919.

609 (20) Muth-Köhne, E.; Sonnack, L.; Schlich, K.; Hischen, F.; Baumgartner, W.; Hund-Rinke,
610 K.; Schäfers, C.; Fenske, M. The Toxicity of Silver Nanoparticles to Zebrafish Embryos
611 Increases through Sewage Treatment Processes. *Ecotoxicology* **2013**, *22* (8), 1264–1277.

612 (21) Kampe, S.; Kaegi, R.; Schlich, K.; Wasmuth, C.; Hollert, H.; Schlechtriem, C. Silver
613 Nanoparticles in Sewage Sludge: Bioavailability of Sulfidized Silver to the Terrestrial
614 Isopod *Porcellio Scaber*. *Environ. Toxicol. Chem.* **2018**, *9999* (9999), 1–8.

615 (22) Kraas, M.; Schlich, K.; Knopf, B.; Wege, F.; Kägi, R.; Terytze, K.; Hund-Rinke, K. Long-
616 Term Effects of Sulfidized Silver Nanoparticles in Sewage Sludge on Soil Microflora.
617 *Environ. Toxicol. Chem.* **2017**, *36* (12), 3305–3313.

618 (23) Pradas del Real, A. E.; Vidal, V.; Carrière, M.; Castillo-Michel, H.; Levard, C.; Chaurand,
619 P.; Sarret, G. Silver Nanoparticles and Wheat Roots: A Complex Interplay. *Environ. Sci.*
620 *Technol.* **2017**, *51* (10), 5774–5782.

621 (24) Laux, P.; Riebeling, C.; Booth, A. M.; Brain, J. D.; Brunner, J.; Cerrillo, C.; Creutzenberg,
622 O.; Estrela-Lopis, I.; Gebel, T.; Johanson, G.; Jungnickel, H.; Kock, H.; Tentschert, J.;
623 Tlili, A.; Schäffer, A.; Sips, A. J. A. M.; Yokel, R. A.; Luch, A. Challenges in
624 Characterizing the Environmental Fate and Effects of Carbon Nanotubes and Inorganic
625 Nanomaterials in Aquatic Systems. *Environ. Sci. Nano* **2017**, *5*, 48–63.

626 (25) Weltje, L.; Sumpter, J. P. What Makes a Concentration Environmentally Relevant?

627 Critique and a Proposal. *Environ. Sci. Technol.* **2017**, *51* (20), 11520–11521.

628 (26) Baker, T. J.; Tyler, C. R.; Galloway, T. S. Impacts of Metal and Metal Oxide
629 Nanoparticles on Marine Organisms. *Environ. Pollut.* **2014**, *186*, 257–271.

630 (27) Joint Research Centre of the European Commission. *Titanium Dioxide, NM-100, NM-101,*
631 *NM-102, NM-103, NM-104, NM-105: Characterisation and Physico- Chemical*
632 *Properties*; 2014.

633 (28) Jensen, K.; Booth, A.; Kembouche, Y.; Boraschi, D. NANoREG Deliverable 2.06.
634 Validated Protocols for Test Item Preparation for Key in Vitro and Ecotoxicity Studies.
635 *NANoREG*. 2016, p 77.

636 (29) Peters, R.; Herrera-Rivera, Z.; Undas, A.; Van Der Lee, M.; Marvin, H.; Bouwmeester,
637 H.; Weigel, S. Single Particle ICP-MS Combined with a Data Evaluation Tool as a
638 Routine Technique for the Analysis of Nanoparticles in Complex Matrices. *J. Anal. At.*
639 *Spectrom.* **2015**, *30*, 1274–1285.

640 (30) International Organisation for Standardization (ISO). Water Quality- Marine Algal
641 Growth Inhibition Test with *Skeletonema Costatum* and *Phaeodactylum Tricornutum* (ISO
642 10253). 2006.

643 (31) Miller, R. J.; Lenihan, H. S.; Muller, E. B.; Tseng, N.; Hanna, S. K.; Keller, A. A. Impacts
644 of Metal Oxide Nanoparticles on Marine Phytoplankton. *Environ. Sci. Technol.* **2010**, *44*
645 (19), 7329–7334.

646 (32) Organisation for Economic Co-operation and Development (OECD). OECD Guidelines

for the Testing of Chemicals/Test 201: Alga, Growth Inhibition Test. **1984**, No. June.

(33) Organisation for Economic Co-operation and Development (OECD). OECD Guidelines for the Testing of Chemicals/ Section 2: Effects on Biotic Systems, Test No. 202: *Daphnia* Sp. Acute Immobilisation Test. **2004**.

(34) Georgantzopoulou, A.; Balachandran, Y. L.; Rosenkranz, P.; Dusinska, M.; Lankoff, A.; Wojewodzka, M.; Kruszewski, M.; Guignard, C.; Audinot, J.-N.; Girija, S.; Hoffmann, L.; Gutleb, A. C. Ag Nanoparticles: Size- and Surface-Dependent Effects on Model Aquatic Organisms and Uptake Evaluation with NanoSIMS. *Nanotoxicology* **2013**, *7* (7), 1168–1178.

(35) United States Environmental Protection Agency. Methods for Measuring the Acute Toxicity of Effluents and Receiving Waters to Freshwater and Marine Organisms. **2002**, No. October, 266.

(36) Macken, A.; Lillicrap, A.; Langford, K. Benzoylurea Pesticides Used as Veterinary Medicines in Aquaculture: Risks and Developmental Effects on Nontarget Crustaceans. *Environ. Toxicol. Chem.* **2015**, *34* (7), 1533–1542.

(37) Schirmer, K.; Chan, A. G. J.; Greenberg, B. M.; Dixon, D. G.; Bols, N. C. Methodology for Demonstrating and Measuring the Photocytotoxicity of Fluoranthene to Fish Cells in Culture. *Toxicol. Vitr.* **1997**, *11* (1–2), 107–119.

(38) Yue, Y.; Behra, R.; Sigg, L.; Fernández Freire, P.; Pillai, S.; Schirmer, K. Toxicity of Silver Nanoparticles to a Fish Gill Cell Line: Role of Medium Composition. *Nanotoxicology* **2015**, *9* (1), 54–63.

668 (39) Hultman, M. T.; Song, Y.; Tollefsen, K. E. 17α-Ethinylestradiol (EE2) Effect on Global
669 Gene Expression in Primary Rainbow Trout (*Oncorhynchus Mykiss*) Hepatocytes. *Aquat.*
670 *Toxicol.* **2015**, *169*, 90–104.

671 (40) Domingos, R. F.; Baalousha, M. A.; Ju-Nam, Y.; Reid, M. M.; Tufenkji, N.; Lead, J. R.;
672 Leppard, G. G.; Wilkinson, K. J. Characterizing Manufactured Nanoparticles in the
673 Environment: Multimethod Determination of Particle Sizes. *Environ. Sci. Technol.* **2009**,
674 *43*, 7277–7284.

675 (41) Wang, Y.; Westerhoff, P.; Hristovski, K. D. Fate and Biological Effects of Silver,
676 Titanium Dioxide, and C 60 (Fullerene) Nanomaterials during Simulated Wastewater
677 Treatment Processes. *J. Hazard. Mater.* **2012**, *201–202*, 16–22.

678 (42) Kim, B.; Park, C. S.; Murayama, M.; Hochella, M. F. Discovery and Characterization of
679 Silver Sulfide Nanoparticles in Final Sewage Sludge Products. *Environ. Sci. Technol.*
680 **2010**, *44* (19), 7509–7514.

681 (43) Gondikas, A. P.; Von Der Kammer, F.; Reed, R. B.; Wagner, S.; Ranville, J. F.; Hofmann,
682 T. Release of TiO2 Nanoparticles from Sunscreens into Surface Waters: A One-Year
683 Survey at the Old Danube Recreational Lake. *Environ. Sci. Technol.* **2014**, *48* (10), 5415–
684 5422.

685 (44) Tuoriniemi, J.; Cornelis, G.; Hassellöv, M. Size Discrimination and Detection Capabilities
686 of Single-Particle ICPMS for Environmental Analysis of Silver Nanoparticles. *Anal.*
687 *Chem.* **2012**, *84* (9), 3965–3972.

688 (45) Mitrano, D. M.; Lesher, E. K.; Bednar, A.; Monserud, J.; Higgins, C. P.; Ranville, J. F.

689 Detecting Nanoparticulate Silver Using Single-Particle Inductively Coupled Plasma-Mass
690 Spectrometry. *Environ. Toxicol. Chem.* **2012**, *31* (1), 115–121.

691 (46) Hadioui, M.; Merdzan, V.; Wilkinson, K. J. Detection and Characterization of ZnO
692 Nanoparticles in Surface and Waste Waters Using Single Particle ICPMS. *Environ. Sci.*
693 *Technol.* **2015**, *49* (10), 6141–6148.

694 (47) Lee, S.; Bi, X.; Reed, R. B.; Ranville, J. F.; Herckes, P.; Westerhoff, P. Nanoparticle Size
695 Detection Limits by Single Particle ICP-MS for 40 Elements. *Environ. Sci. Technol.* **2014**,
696 *48* (17), 10291–10300.

697 (48) Mallevre, F.; Alba, C.; Milne, C.; Gillespie, S.; Fernandes, T.; Aspray, T. Toxicity Testing
698 of Pristine and Aged Silver Nanoparticles in Real Wastewaters Using Bioluminescent
699 *Pseudomonas Putida*. *Nanomaterials* **2016**, *6* (3), 49.

700 (49) Saison, C.; Perreault, F.; Daigle, J. C.; Fortin, C.; Claverie, J.; Morin, M.; Popovic, R.
701 Effect of Core-Shell Copper Oxide Nanoparticles on Cell Culture Morphology and
702 Photosynthesis (Photosystem II Energy Distribution) in the Green Alga, *Chlamydomonas*
703 *Reinhardtii*. *Aquat. Toxicol.* **2010**, *96* (2), 109–114.

704 (50) Oukarroum, A.; Bras, S.; Perreault, F.; Popovic, R. Inhibitory Effects of Silver
705 Nanoparticles in Two Green Algae, *Chlorella Vulgaris* and *Dunaliella Tertiolecta*.
706 *Ecotoxicol. Environ. Saf.* **2012**, *78*, 80–85.

707 (51) Zaytseva, O.; Neumann, G. Carbon Nanomaterials: Production, Impact on Plant
708 Development, Agricultural and Environmental Applications. *Chem. Biol. Technol. Agric.*
709 **2016**, *3* (1), 17.

710 (52) Taylor, C.; Matzke, M.; Kroll, A.; Read, D. S.; Svendsen, C.; Crossley, A. Toxic
711 Interactions of Different Silver Forms with Freshwater Green Algae and Cyanobacteria
712 and Their Effects on Mechanistic Endpoints and the Production of Extracellular Polymeric
713 Substances. *Environ. Sci. Nano* **2016**, *3* (2), 396–408.

714 (53) Levard, C.; Hotze, E. M.; Colman, B. P.; Dale, A. L.; Truong, L.; Yang, X. Y.; Bone, A.
715 J.; Brown, G. E.; Tanguay, R. L.; Di Giulio, R. T.; Bernhardt, E. S.; Meyer, J. N.;
716 Wiesner, M. R.; Lowry, G. V. Sulfidation of Silver Nanoparticles: Natural Antidote to
717 Their Toxicity. *Environ. Sci. Technol.* **2013**, *47* (23), 13440–13448.

718 (54) Gophen, M.; Geller, W. Filter Mesh Size and Food Particle Uptake by *Daphnia*.
719 *Oecologia* **1984**, *64* (3), 408–412.

720 (55) Williams, T. Survival and Development of Copepod Larvae *Tisbe Battagliai* in Surface
721 Microlayer, Water and Sediment Elutriates from the German Bight. *Mar. Ecol. Prog. Ser.*
722 **1992**, *91*, 221–228.

723 (56) Puello□Cruz, A. C.; Mezo□Villalobos, S.; Voltolini, D. Progeny Production of the
724 Copepods *Pseudodiaptomus Euryhalinus* and *Tisbe Monozota* in Monospecific and Mixed
725 Cultures. *J. world Aquac. Soc.* **2013**, *44* (3), 447–454.

726 (57) Liu, J.; Hurt, R. H. Ion Release Kinetics and Particle Persistence in Aqueous Nano-Silver
727 Colloids. *Environ. Sci. Technol.* **2010**, *44* (6), 2169–2175.

728 (58) Loza, K.; Diendorf, J.; Sengstock, C.; Ruiz-Gonzalez, L.; Gonzalez-Calbet, J. M.; Vallet-
729 Regi, M.; Köller, M.; Epple, M. The Dissolution and Biological Effects of Silver
730 Nanoparticles in Biological Media. *J. Mater. Chem. B* **2014**, *2* (12), 1634.

731 (59) Navarro, E.; Piccapietra, F.; Wagner, B.; Marconi, F.; Kaegi, R.; Odzak, N.; Sigg, L.;
732 Behra, R. Toxicity of Silver Nanoparticles to *Chlamydomonas Reinhardtii*. *Environ. Sci.*
733 *Technol.* **2008**, *42* (23), 8959–8964.

734 (60) Zhao, C.-M.; Wang, W.-X. Comparison of Acute and Chronic Toxicity of Silver
735 Nanoparticles and Silver Nitrate to *Daphnia Magna*. *Environ. Toxicol. Chem.* **2011**, *30*
736 (4), 885–892.

737 (61) Köser, J.; Engelke, M.; Hoppe, M.; Nogowski, A.; Filser, J.; Thöming, J. Predictability of
738 Silver Nanoparticle Speciation and Toxicity in Ecotoxicological Media. *Environ. Sci.*
739 *Nano* **2017**, *4* (7), 1470–1483.

740 (62) Bury, N. R.; Schnell, S.; Hogstrand, C. Gill Cell Culture Systems as Models for Aquatic
741 Environmental Monitoring. *J. Exp. Biol.* **2014**, *217*, 639–650.

742 (63) Lee, L. E. J.; Dayeh, V. R.; Schirmer, K.; Bols, N. C. Applications and Potential Uses of
743 Fish Gill Cell Lines: Examples with RTgill-W1. *Vitr. Cell. Dev. Biol. - Anim.* **2009**, *45* (3–
744 4), 127–134.

745 (64) Minghetti, M.; Schnell, S.; Chadwick, M. A.; Hogstrand, C.; Bury, N. R. A Primary FIsh
746 Gill Cell System (FIGCS) for Environmental Monitoring of River Waters. *Aquat. Toxicol.*
747 **2014**, *154*, 184–192.

748 (65) Walker, P. A.; Kille, P.; Hurley, A.; Bury, N. R.; Hogstrand, C. An *in Vitro* Method to
749 Assess Toxicity of Waterborne Metals to Fish. *Toxicol. Appl. Pharmacol.* **2008**, *230* (1),
750 67–77.

751 (66) Farkas, J.; Christian, P.; Gallego-Urrea, J. A.; Roos, N.; Hassellöv, M.; Tollefsen, K. E.;
752 Thomas, K. V. Uptake and Effects of Manufactured Silver Nanoparticles in Rainbow
753 Trout (*Oncorhynchus Mykiss*) Gill Cells. *Aquat. Toxicol.* **2011**, *101* (1), 117–125.

754 (67) Trubitt, R. T.; Rabeneck, D. B.; Bujak, J. K.; Bossus, M. C.; Madsen, S. S.; Tipsmark, C.
755 K. Transepithelial Resistance and Claudin Expression in Trout RTgill-W1 Cell Line:
756 Effects of Osmoregulatory Hormones. *Comp. Biochem. Physiol. -Part A Mol. Integr.*
757 *Physiol.* **2015**, *182*, 45–52.

758 (68) Meyer, T. N.; Schwesinger, C.; Ye, J.; Denker, B. M.; Nigam, S. K. Reassembly of the
759 Tight Junction after Oxidative Stress Depends on Tyrosine Kinase Activity. *J. Biol. Chem.*
760 **2001**, *276* (25), 22048–22055.

761 (69) Georgantzopoulou, A.; Cambier, S.; Serchi, T.; Kruszewski, M.; Balachandran, Y. L.;
762 Grysan, P.; Audinot, J. N.; Ziebel, J.; Guignard, C.; Gutleb, A. C.; Murk, A. T. J.
763 Inhibition of Multixenobiotic Resistance Transporters (MXR) by Silver Nanoparticles and
764 Ions *in Vitro* and in *Daphnia Magna*. *Sci. Total Environ.* **2016**, *569–570* (0349), 681–689.

765 (70) Wu, B.; Torres-Duarte, C.; Cole, B. J.; Cherr, G. N. Copper Oxide and Zinc Oxide
766 Nanomaterials Act as Inhibitors of Multidrug Resistance Transport in Sea Urchin
767 Embryos: Their Role as Chemosensitizers. *Environ. Sci. Technol.* **2015**, *49*, 5760–5770.

768 (71) Yang, Y.; Wang, Y.; Westerhoff, P.; Hristovski, K.; Jin, V. L.; Johnson, M. V. V; Arnold,
769 J. G. Metal and Nanoparticle Occurrence in Biosolid-Amended Soils. *Sci. Total Environ.*
770 **2014**, *485–486* (1), 441–449.

771

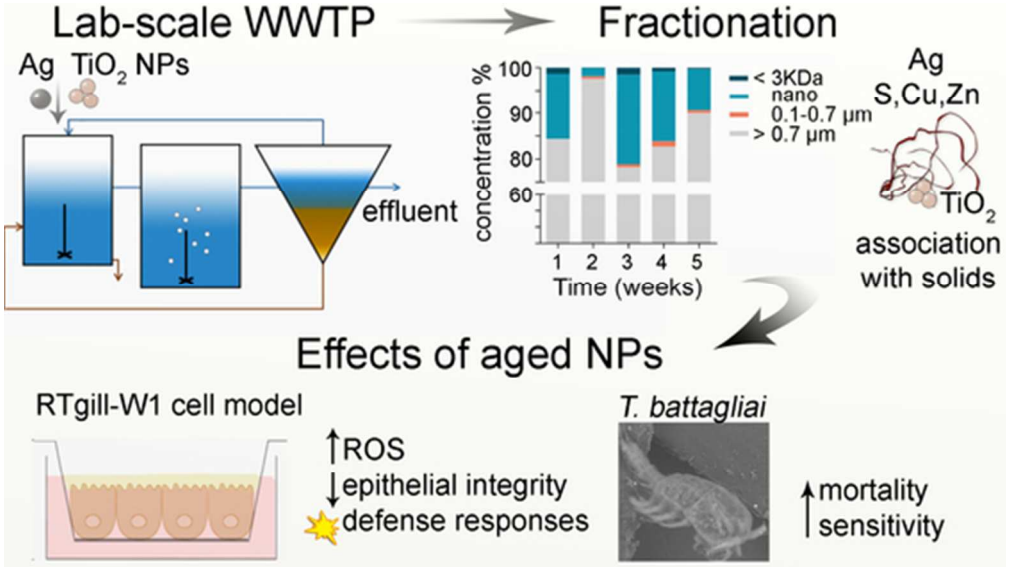

Graphical abstract

47x26mm (300 x 300 DPI)